Protein–DNA Arrays

Engineering a 2D Protein–DNA Crystal**

*Jonathan Malo, James C. Mitchell, Catherine Vénien-Bryan, J. Robin Harris, Holger Wille, David J. Sherratt, and Andrew J. Turberfield**

Here, we demonstrate the use of a DNA-binding protein to control the structure of a self-assembled DNA crystal. DNA self-assembly[1] has been used to create a variety of nanometer-scale objects including polyhedra,[2] simple machines,[3] two-dimensional arrays,[4] and periodic tubes.[5] Controlled construction by self-assembly is possible because the pattern of hybridization between complementary sections of oligo-

[*] J. Malo,[+] Dr. J. C. Mitchell,[+] Prof. A. J. Turberfield
Department of Physics, Clarendon Laboratory
University of Oxford, Parks Road, Oxford OX1 3PU (UK)
Fax: (+44) 1865-272-400
E-mail: a.turberfield@physics.ox.ac.uk

Dr. C. Vénien-Bryan[+]
Laboratory of Molecular Biophysics
Department of Biochemistry
University of Oxford, South Parks Road, Oxford OX1 3QU (UK)

J. Malo,[+] Prof. D. J. Sherratt
Department of Biochemistry
University of Oxford, South Parks Road, Oxford OX1 3QU (UK)

Prof. J. R. Harris
Institute of Zoology
University of Mainz, 55099 Mainz (Germany)

Prof. H. Wille
Department of Neurology and
Institute for Neurodegenerative Diseases
University of California, San Francisco, CA 94143 (USA)

[+] These authors contributed equally to this work.

[**] This work was supported by the Wellcome Trust, the MoD, and the UK research councils BBSRC, EPSRC, and MRC through the UK Bionanotechnology IRC. We thank Prof. Louise Johnson of the Laboratory of Molecular Biophysics, Oxford, for her advice, and Prof. Werner Kuhlbrandt, Dr. Janet Vonck, and Mr. Deryck Mills of the MPI for Biophysics, Frankfurt, for the use of their cryo-EM facilities and for their assistance in the cryo-EM imaging of the RuvA–HJ lattices.

Supporting information for this article is available on the WWW under http://www.angewandte.org or from the author.

 DOI: 10.1002/ange.200463027

nucleotides can be predicted. Additional control can be achieved by making use of the wide range of proteins that have evolved to manipulate DNA in order to maintain and replicate genetic information. Of these, ligases and nucleases have been used during the process of DNA nanostructure fabrication and characterization to make chemical modifications to the phosphodiester backbone.[2,4a,b,d,g] Here, we report the incorporation of a bacterial recombination protein, RuvA, as an *intrinsic* component of a DNA nanostructure. By analyzing transmission electron micrographs we have produced 2D density maps (maps of transmitted electron intensity) of both RuvA–DNA and DNA-only crystals to resolutions of less than 30 Å. Both crystals are built from the same four oligonucleotides: addition of RuvA during self-assembly completely changes the lattice symmetry and connectivity. Such specially designed 2D DNA templates, used to create ordered protein arrays, may provide a tool to determine the structure of proteins that do not readily crystallize.

Our DNA arrays are built from four oligonucleotides that assemble, by hybridization of complementary sections, to form the four arms of an immobile Holliday junction (HJ)[6] shown in Figure 1 a. Each arm has a "sticky end" that consists of six unpaired bases. Each sticky end is complementary to one other; complementary sticky ends are indicated by lock-and-key symbols in Figure 1 b and e (red pairs with green, yellow pairs with blue). Hybridization of sticky ends can bind the junctions together to form an extended array. The Kagome[7] lattice shown in Figure 1 c and d consists of DNA only and is assembled by slowly cooling a stoichiometric mixture of the four oligonucleotides from 90 °C to 20 °C over 72 h. Figure 1 d shows a transmission electron micrograph of this structure, positively stained[8] with 2 % uranyl acetate. The HJs adopt a stable antiparallel χ-stacked configuration,[9] shown schematically in Figure 1 b. Pairs of arms stack coaxially to form two quasi-continuous double helices, which meet at approximately 60° in a right-handed cross. The red and orange oligonucleotides run continuously from end to end of the two double helices with largely unperturbed helical structure; the other two oligonucleotides (green and blue) cross between helices where they meet to hold the junction together. Hybridization of complementary sticky ends joins the arms of the junctions together to form extended helices. Adjacent junctions are separated by 26 base pairs or 2.5 DNA helical turns. Three sets of parallel helices are interwoven as in Kagome basketwork (Figure 1 c), with each helix woven alternately above and below others that cross at 60° and 120°. The helices must bend as they weave, which suggests a structure with kinks at the ends of the six-base sections where sticky ends overlap to reduce the resultant strain. The plane group of the crystal is *p*3 (sixfold rotational symmetry is broken by differences between the base sequences of neighboring helices that flank the hexagons and in the positions of the nicks in the DNA backbones where sticky ends overlap). A primitive unit cell contains three junctions. Only the HJ isomer shown in Figure 1 b can be incorporated into this lattice. In the other antiparallel χ-stacked isomer, in which the blue and green oligonucleotides run continuously through the junction, complementary pairs of sticky ends are on opposite rather than adjacent arms; this isomer may assemble to create a three-dimensional periodic structure.

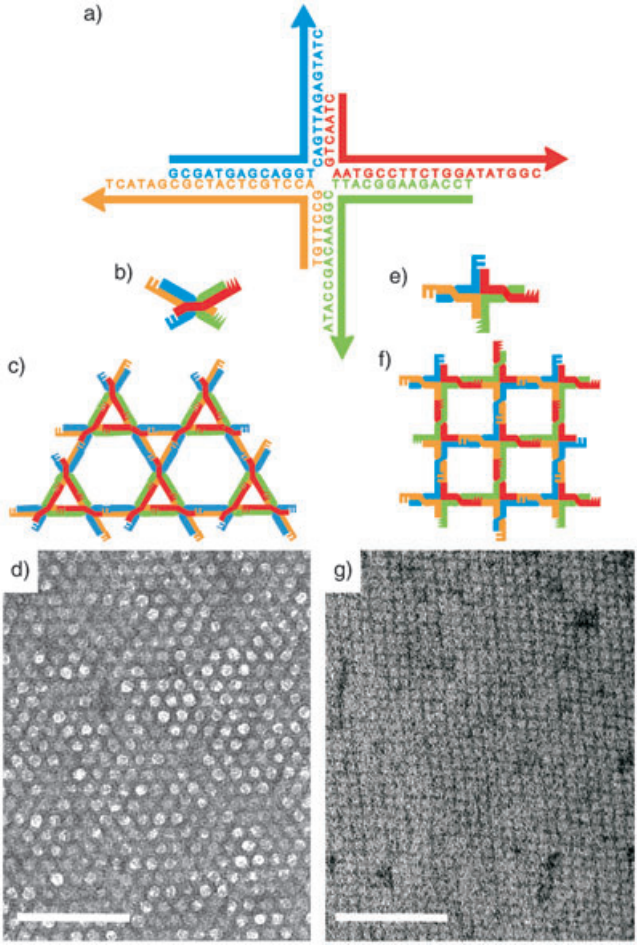

Figure 1. DNA crystals: a) The common structural unit—four oligonucleotides hybridize to form a Holliday junction (HJ) with two pairs of complementary "sticky ends". b) χ-stacked junction showing the positions of complementary sticky ends. c) Kagome lattice formed by assembly of χ-stacked junctions (for clarity, half a helical turn is shown between junctions that are, in fact, separated by 2.5 turns). d) TEM (transmission electron microscopy) image of the Kagome lattice (DNA is positively stained (dark); scale bar: 100 nm). e) Square-planar junction. f) Square lattice formed from HJs held in a square-planar configuration by protein RuvA. g) TEM image of the RuvA lattice (negatively stained: protein is lighter than background; scale bar: 100 nm).

The formation of the DNA crystal from its component oligonucleotides can be followed by measuring the decrease in A_{260}, the absorbance at 260 nm, as the mixture is slowly cooled. (A_{260} decreases as oligonucleotides hybridize.[10]) Figure 2 a shows A_{260} as a function of temperature as stoichiometric mixtures of oligonucleotides are slowly annealed and then melted. The lower pair of curves correspond to four oligonucleotides synthesized without the sticky ends that hold the junctions together. Dotted lines at 63 °C and 38 °C mark the calculated transition temperatures[11] for the assembly steps shown in Figure 2 b: first the hybridization of pairs of oligonucleotides that form the two long arms of the junction, then the coming together of these pairs to form the junction. Cooling and melting curves are overlaid, and no

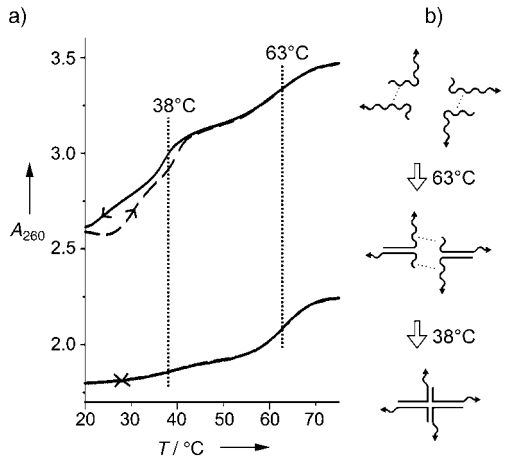

Figure 2. Monitoring self-assembly by UV/Vis absorbance spectroscopy. a) Absorbance at 260 nm (A_{260}) as a function of temperature (T) during assembly (——) and melting (-----). Hybridization is associated with a decrease in absorbance. Plots correspond to a 3 μM stoichiometric mixture of the four oligonucleotides shown in Figure 1a (upper curves) and of the same oligonucleotides with the four sticky ends removed to prevent array formation (lower curves). Rate of change of temperature: 0.1 °C min^{-1}. Dotted lines (•••••) indicate calculated transition temperatures corresponding to the assembly steps shown in part (b).

significant hysteresis is observed. The upper curves correspond to assembly and melting of the four oligonucleotides with sticky ends shown in Figure 1a. Reversible assembly of the longer arms at 63 °C is again observed, but below 42 °C there is rate-dependent hysteresis that we associate with the hybridization of sticky ends to assemble extended arrays with the structure shown in Figure 1c and d. We conclude that, as the reactants are cooled, the two more-stable pairs of oligonucleotides hybridize first then array formation begins as soon as these pairs combine to form complete junctions. This is consistent with the observation that slow cooling in the range 40–20 °C improves the size and crystalline order of the arrays, whereas slow cooling at higher temperatures does not.

The crystal shown in Figure 1f and g is made from the same four oligonucleotides to form the same HJ. In this case, however, the structure also incorporates RuvA. In vivo RuvA is part of a tripartite protein complex, the RuvABC "resolvasome",[12] which processes Holliday junctions[13] during bacterial homologous recombination. RuvA has a natural architectural role: it holds the HJ in a square-planar configuration that facilitates branch migration, driven by the ATPase RuvB,[14] and allows resolution by the endonuclease RuvC.[15] Holliday junctions are the building blocks of our DNA arrays: when RuvA binds to them during self-assembly it plays a decisive role in determining the structure and symmetry of the array. The protein is added to the cooling solution of oligonucleotides at 50 °C, at which temperature HJs have not yet formed. RuvA binds to the isolated HJs and unfolds them into a square-planar configuration[16,17] (Figure 1e). The angles between the arms are approximately 90°, the arms do not stack to form continuous helices, and the ordering of the sticky ends is different from the χ-stacked configuration (all four oligonucleotides turn at the junction to run along adjacent arms). The effect is dramatic. On further cooling the weak interactions between sticky ends assemble the units into a square lattice. In Figure 1g contrast is provided by 2% uranyl acetate which negatively stains the RuvA protein that binds each HJ.[18] The plane group of the crystal is $p1$. A primitive unit cell contains two junctions with different orientations, one of which has the major groove side upwards, and the other downwards. The connectivities of the two lattices, square and Kagome, are such that they cannot be interconverted without breaking the bonds between sticky ends that hold HJs together. Addition of RuvA at 20 °C to a ready-formed Kagome lattice does not cause detectable conversion to a square lattice.

For both crystal types, ordered domains up to 2 μm in size are observed in TEM images. Contrast between DNA or protein and background, even in the stained images shown in Figure 1d and g, is low, and the signal-to-noise ratio is limited by the need to use low electron-beam current densities to avoid damage. To obtain higher resolution structural information we have adopted two approaches to combine data from many unit cells: a process of iterative correlation mapping and averaging[19] based on the SPIDER and WEB single-particle imaging software,[20] and correction for distortion of the crystal lattice followed by reciprocal-space analysis using the MRC image-processing suite[21] designed for periodic structures. Projected density maps derived by using SPIDER are shown in Figure 3 and Figure 4 and are compared with the output of the MRC suite in the Supporting Information.

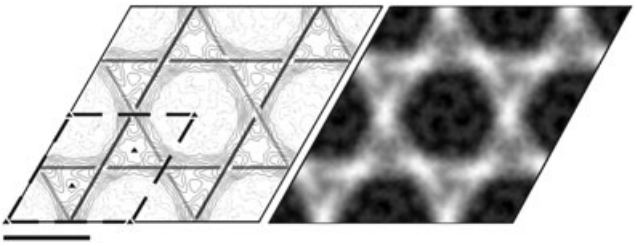

Figure 3. 2D-projected density map of a Kagome lattice composed of three interwoven DNA helices joined by χ-stacked Holliday junctions (scale bar: 10 nm). The map is derived from a negatively stained TEM image of a self-assembled DNA crystal. The contour plot and grayscale images represent the same data; woven lines indicate the positions of the helices. Dashed lines delineate a unit cell annotated with $p3$ plane group symmetry elements.

Figure 3 shows a projected density map of the DNA-only Kagome lattice. Ellipsoidal regions of high density reveal the positions of the χ-stacked HJs. The alternating orientations of the ellipses are consistent with the Kagome weaving of the helices indicated by lines in Figure 3. The distance between the junctions is 72 Å, which is 16 Å less than the contour length of the DNA duplex that joins them. We expect this distance to be shortened by strain-relieving kinks at nicks in the DNA backbone at either end of the 20 Å section that corresponds to the hybridized sticky ends. Shrinkage of the DNA caused by dehydration during grid preparation[22] may also affect this measurement.

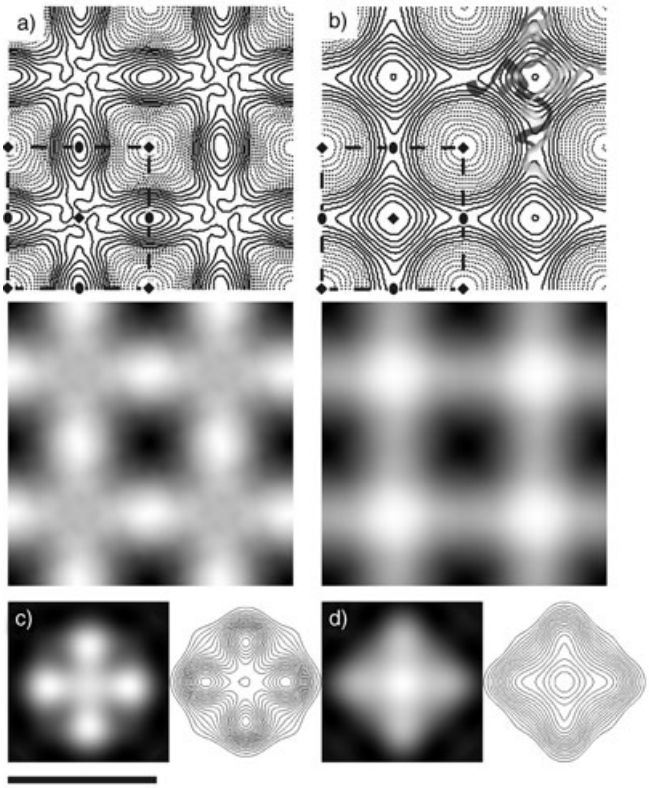

Figure 4. a, b) Projected density maps of two RuvA–DNA crystals derived from cryo-electron micrographs. Each map is represented by both a contour plot and a grayscale image. Dashed lines delineate a unit cell annotated with *p*4 plane group symmetry elements. A section of the DNA template that provides structural order is shown for illustration only. For comparison we show projection maps derived from X-ray crystal structures of Holliday junctions bound by c) a tetramer and d) an octamer of RuvA (see Supporting Information). Scale bar: 10 nm.

The protein and DNA components of the RuvA–DNA crystal shown in Figure 1g have different affinities for the uranyl acetate stain: positive staining of the DNA distorts the outline of the negatively stained RuvA complex that binds each HJ. We obtained undistorted images of this composite structure by using cryo-electron microscopy (cryo-EM) in which a thin layer of vitreous ice preserves the hydrated structure, and the image is generated by the density difference between protein and ice.[2d,23] Figure 4a and b show maps of the projected densities obtained from two RuvA–DNA crystals prepared in this way. No difference between the two differently oriented HJs in the unit cell can be resolved, so the averaged projection map has a smaller and more symmetrical unit cell than the crystal itself. The primitive unit cells of the images shown in Figure 4a and b contain one HJ and have *p*4 symmetry ($a = 95$ and 97 Å for Figure 4a and b, respectively). In Figure 4c and d, we show for comparison projected density maps derived from the X-ray crystal structures of the two known RuvA–HJ complexes, one of which incorporates a RuvA tetramer bound to one face of the junction,[16b] and the other an octamer with four molecules of RuvA bound to each face.[17] These maps have been filtered to give a resolution that is comparable to that of the cryo-EM data. The correspondence between our measured projection maps and the X-ray crystal structures is striking. We tentatively conclude that in the crystals from which the projection maps shown in Figure 4a and b were derived, which were prepared under nominally the same conditions, most HJs were bound by RuvA tetramers and octamers, respectively.

The structure of self-assembled 2D DNA crystals has previously been investigated by atomic force microscopy[4] with resolution limited to about 70 Å.[4c] To enhance the visibility of the lattice it was found necessary to add topographic features such as protruding hairpins, larger DNA domains, or streptavidin bound to biotinylated oligonucleotides,[4a,d,f,g] or to design structures with large, easily resolved gaps.[4b,c,e,h] Our micrographs demonstrate that transmission electron microscopy can provide significantly higher resolution. From computed Fourier transforms, and by comparison with the known X-ray crystal structures of the RuvA–HJ complex, we estimate the resolution of Figure 3 and Figure 4a and b to lie between 25 and 30 Å.

The use of three-dimensional DNA scaffolds[24] as templates to create artificial protein crystals for X-ray crystallography has been proposed by Seeman.[25] The structure shown in Figure 1g and Figure 4 may be regarded as a two-dimensional protein crystal whose structural order is provided by the underlying DNA scaffold rather than by interactions between protein molecules. Our density map of the RuvA–HJ complex demonstrates that a DNA-templated protein crystal can be produced with sufficient spatial order to allow measurement of protein structure. Electron microscopy of 2D crystals has achieved resolutions of 3.5 Å[26] and has the advantage that very small quantities of protein are required (typically of order 1 μg per grid). We are now working to attain higher resolution maps by improving the quality of our crystals and aim to extend the application of the DNA-scaffolding method to produce artificial crystals of other proteins, including membrane proteins that are bound to ligands attached to covalently modified oligonucleotides in a self-assembled DNA array.

Experimental Section

Purification of *E. coli* RuvA: A strain of GS566 *E. coli* that contains a RuvA-producing, ampicillin-resistant plasmid was provided by Dr. Matthew Whitby, University of Oxford. Cells were grown to OD ≈ 0.5 at 30 °C over 4 h followed by temperature-sensitive induction at 42 °C for 5 h. After lysis by sonication, purification by a series of three alternate fast-performance liquid chromatography and dialysis steps were performed to yield a solution of RuvA (80 μM, ≈ 12 mg l^{-1} of induced culture). See Supporting Information for further details.

Crystal design and assembly: Oligonucleotide sequences were designed using the program SEQUIN[27] around a symmetric sequence flanking the Holliday junction.[28] For construction of the DNA-only Kagome lattice, a stoichiometric (3 μM) mixture of the four component oligonucleotides (Sigma-Genosys; Figure 1a) was cooled from 90 °C to 20 °C over approximately 72 h in annealing buffer 1 ($MgCl_2$ (30 mM)/Tris·HCl (5 mM)/Tris acetate (20 mM)/EDTA (1 mM), pH 8.3) using a Mastercycler PCR machine (Eppendorf). The DNA–RuvA crystals were annealed using the same oligonucleotides at the same concentration in annealing buffer 2 ($MgCl_2$ (10 mM)/Tris·HCl (10 mM)/Tris acetate (40 mM)/EDTA

(1 mM), pH 8.3), also over approximately 72 h. The sample container was immersed in water in a vacuum flask, which was left to cool naturally. RuvA (24 μM) was added at 50 °C.

UV/Vis absorbance measurements: A Varian Cary 1E spectrophotometer with a 6x6 multicell-block Peltier temperature controller was used to measure the differential absorbance (A) at 260 nm between the sample, which contained a mixture of the four component oligonucleotides (3 μM) in annealing buffer 1, and a reference (only annealing buffer), both at 650 μl volume. The temperature was measured by a probe placed in a third cuvette.

Preparation of grids and electron microscopy: Specimens of the Kagome lattice were adsorbed onto 400-mesh carbon-coated copper grids and stained with 2% uranyl acetate. Electron micrographs were recorded on Kodak SO-163 film under low dose conditions using a Philips CM120 electron microscope (LMB, Oxford) at 120 kV acceleration. The defocus range was from 0.6 to 1.2 μm with a nominal magnification of ×45000. RuvA–DNA crystal specimens were applied to carbon-coated grids initially immersed in 1% tannin. These were then blotted and frozen in liquid nitrogen. Electron micrographs were recorded under low dose conditions on a JEOL 3000 electron microscope (MPI, Frankfurt) at 300 kV acceleration. The defocus range was from 0.6 to 1.2 μm with a nominal magnification of ×36000.

Image processing: Optical diffraction was used to screen and select the micrographs for crystal quality. The Kagome lattice projection map (Figure 3) was calculated from one large crystalline area ($\approx 0.6\ \mu m^2$) of an image in which the DNA was negatively stained.[18] (This image is more ordered but displays less contrast than Figure 1d in which the DNA is positively stained.[8]) The RuvA–DNA projection maps (Figure 4) were calculated using data from two separate crystals imaged under cryo-EM. Selected areas were digitized using an Optronics drum scanner (P1000) at a sampling raster of 12.5 μm that corresponds to a pixel size of 2.8 Å. A contrast transfer function (CTF) correction was applied using the CRISP software package.[29] The CTF-corrected images were processed by using correlation mapping and averaging routines[19] written for the SPIDER and WEB software packages.[20] See Supporting Information for further details.

Received: December 22, 2004
Published online: April 12, 2005

Keywords: DNA · electron microscopy · nanostructures · proteins · self-assembly

[1] N. C. Seeman, *Nature* **2003**, *421*, 427.
[2] a) J. H. Chen, N. C. Seeman, *Nature* **1991**, *350*, 631; b) Y. W. Zhang, N. C. Seeman, *J. Am. Chem. Soc.* **1994**, *116*, 1661; c) R. P. Goodman, R. M. Berry, A. J. Turberfield, *Chem. Commun.* **2004**, *12*, 1372; d) W. M. Shih, J. D. Quispe, G. F. Joyce, *Nature* **2004**, *427*, 618.
[3] a) B. Yurke, A. J. Turberfield, A. P. Mills, Jr., F. C. Simmel, J. L. Neumann, *Nature* **2000**, *406*, 605; b) H. Yan, X. Zhang, Z. Shen, N. C. Seeman, *Nature* **2002**, *415*, 62.
[4] a) E. Winfree, F. Liu, L. A. Wenzler, N. C. Seeman, *Nature* **1998**, *394*, 539; b) C. D. Mao, W. Q. Sun, N. C. Seeman, *J. Am. Chem. Soc.* **1999**, *121*, 5437; c) R. Sha, F. Liu, D. P. Millar, N. C. Seeman, *Chem. Biol.* **2000**, *7*, 743; d) T. H. LaBean, H. Yan, J. Kopatsch, F. R. Liu, E. Winfree, J. H. Reif, N. C. Seeman, *J. Am. Chem. Soc.* **2000**, *122*, 1848; e) R. Sha, F. Liu, N. C. Seeman, *Biochemistry* **2002**, *41*, 5950; f) H. Yan, S. H. Park, G. Finkelstein, J. H. Reif, T. H. LaBean, *Science* **2003**, *301*, 1882; g) H. Yan, T. H. LaBean, L. Feng, J. H. Reif, *Proc. Natl. Acad. Sci. USA* **2003**, *100*, 8103; h) L. Feng, S. H. Park, J. H. Reif, H. Yan, *Angew. Chem.* **2003**, *115*, 4478; *Angew. Chem. Int. Ed.* **2003**, *42*, 4342.
[5] a) J. C. Mitchell, J. R. Harris, J. Malo, J. Bath, A. J. Turberfield, *J. Am. Chem. Soc.* **2004**, *126*, 16342; b) P. W. K. Rothemund, E. Ekani-Nkodo, N. Papadakis, A. Kumar, D. K. Fygenson, E. Winfree, *J. Am. Chem. Soc.* **2004**, *126*, 16344.
[6] N. R. Kallenbach, R.-I. Ma, N. C. Seeman, *Nature* **1983**, *305*, 829.
[7] I. Syôzi, *Prog. Theor. Phys.* **1951**, *6*, 306.
[8] M. Beer, C. R. Zobel, *J. Mol. Biol.* **1961**, *3*, 717.
[9] a) M. Ortiz-Lombardia, A. Gonzalez, R. Eritja, J. Aymami, F. Azorin, M. Coll, *Nat. Struct. Biol.* **1999**, *6*, 913; b) B. F. Eichman, J. M. Vargason, B. H. Mooers, P. S. Ho, *Proc. Natl. Acad. Sci. USA* **2000**, *97*, 3971.
[10] R. Thomas, *Biochim. Biophys. Acta* **1954**, *14*, 231.
[11] a) N. Peyret, P. A. Seneviratne, H. T. Allawi, J. SantaLucia, Jr., *Biochemistry* **1999**, *38*, 3468; b) J. SantaLucia, Jr., *Proc. Natl. Acad. Sci. USA* **1998**, *95*, 1460.
[12] D. Zerbib, C. Mezard, H. George, S. C. West, *J. Mol. Biol.* **1998**, *281*, 621.
[13] R. Holliday, *Genet. Res.* **1964**, *5*, 282.
[14] A. Stasiak, I. R. Tsaneva, S. C. West, C. J. Benson, X. Yu, E. H. Egelman, *Proc. Natl. Acad. Sci. USA* **1994**, *91*, 7618.
[15] M. Ariyoshi, D. G. Vassylyev, H. Iwasaki, H. Nakamura, H. Shinagawa, K. Morikawa, *Cell* **1994**, *78*, 1063.
[16] a) D. Hargreaves, D. W. Rice, S. E. Sedelnikova, P. J. Artymiuk, R. G. Lloyd, J. B. Rafferty, *Nat. Struct. Biol.* **1998**, *5*, 441; b) M. Ariyoshi, T. Nishino, H. Iwasaki, H. Shinagawa, K. Morikawa, *Proc. Natl. Acad. Sci. USA* **2000**, *97*, 8257.
[17] S. M. Roe, T. Barlow, T. Brown, M. Oram, A. Keeley, I. R. Tsaneva, L. H. Pearl, *Mol. Cell* **1998**, *2*, 361.
[18] R. W. Horne in *Techniques for Electron Microscopy* (Ed.: D. H. Kay), Blackwell Scientific Publishing, Oxford, **1965**, pp. 328.
[19] H. Wille, M. D. Michelitsch, V. Guenebaut, S. Supattapone, A. Serban, F. E. Cohen, D. A. Agard, S. B. Prusiner, *Proc. Natl. Acad. Sci. USA* **2002**, *99*, 3563.
[20] J. Frank, M. Radermacher, P. Penczek, J. Zhu, Y. Li, M. Ladjadj, A. Leith, *J. Struct. Biol.* **1996**, *116*, 190.
[21] R. A. Crowther, R. Henderson, J. M. Smith, *J. Struct. Biol.* **1996**, *116*, 9.
[22] H. J. Vollenweider, A. James, W. Szybalski, *Proc. Natl. Acad. Sci. USA* **1978** *75*, 710; G. Lee, P. G. Arscott, V. A. Bloomfield, D. F. Evans, *Science* **1989**, *244*, 475.
[23] M. Adrian, J. Dubochet, J. Lepault, A. W. McDowall, *Nature* **1984**, *308*, 32.
[24] P. J. Paukstelis, J. Nowakowski, J. J. Birktoft, N. C. Seeman, *Chem. Biol.* **2004**, *11*, 1119.
[25] N. C. Seeman, *J. Theor. Biol.* **1982**, *99*, 237.
[26] R. Henderson, J. M. Baldwin, T. A. Ceska, F. Zemlin, E. Beckmann, K. H. Downing, *J. Mol. Biol.* **1990**, *213*, 899.
[27] N. C. Seeman, *J. Biomol. Struct. Dyn.* **1990**, *8*, 573.
[28] S. Zhang, N. C. Seeman, *J. Mol. Biol.* **1994**, *238*, 658.
[29] S. Hovmöller, *Ultramicroscopy* **1992**, *41*, 121.

